GEOLOGIJA *52/1*, 21-28, Ljubljana 2009

Volcanic succession of the Borovnik Member (Mohorje Formation), Bloke Plateau area, Central Slovenia

Vulkanske kamnine Borovniškega člena Mohorske formacije na območju Bloške planote

Polona KRALJ & Stevo DOZET

Geological Survey of Slovenia, Dimičeva ul. 14, SI-1000 Ljubljana, Slovenija
e-mail: p.kralj@geo-zs.si; stevo.dozet@geo-zs.si

Prejeto / Received 3. 11. 2008; Sprejeto / Accepted 12. 11. 2008

Key words: Triassic volcanism, dacitic rocks, peperites, submarine volcaniclastics, Borovnik Member, Mohorje Formation, Central Slovenia
Ključne besede: triasni vulkanizem, dacitne kamnine, peperiti, podmorski vulkanoklastiti, Borovniški člen, Mohorska formacija, osrednja Slovenija

Abstract

A 75 m thick volcanic succession of the Borovnik Member, Mohorje Formation in the Bloke Plateau area consists of dacitic and rhyolitic rocks deposited in a shallow-marine environment. Volcanic activity begun with lava flows that underwent extensive disintegration, autobrecciation and mixing with the underlying unconsolidated fine-grained clastic sediments producing dacite/rhyolite-siltstone peperites. Peperites are very rich in fractured plagioclase phenocrysts, and owing to the incorporation of clastic material, they are commonly depleted in silica. The overlying fining-upward pyroclastic sequence is monotonous. Basal parts mainly consist of coarse-grained vitric tuffs that may contain some smaller pumice lapilli. The overlying volcaniclastics are fine-grained vitric tuffs, and in the uppermost parts of the sequence, they are interbedded with cherts.

The study confirms the existence of primary volcaniclastic succession in the Bloke Plateau area and excludes its epiclastic or reworked origin.

Izvleček

75 m debelo vulkansko zaporedje Borovniškega člena Mohorske formacije na območju Bloške planote sestoji iz dacitnih in riolitnih kamnin, ki so ekstrudirale v plitvo morsko okolje. Vulkanska aktivnost se je pričela z izlivi lave, ki so se zaradi ohlajanja močno drobili, avtobrečirali in mešali z drobnozrnatim sedimentom podlage ter ustvarjali peperite dacita/riodacita in meljevca. Peperiti so bogati z vtrošniki plagioklazov, ki so močno razpokani, zaradi vsebnosti klastičnega nevulkanskega materiala pa so pogosto revnejši s kremenico. Nad peperiti leži zaporedje monotono debelozrnatih in drobnozrnatih tufov z zmanjševanjem zrnavosti navzgor. Spodnji del zaporedja sestoji iz debelozrnatih vitričnih tufov, ki vsebujejo tudi manjše lapile plovca, nad njimi pa leže drobnozrnati vitrični tufi, ki se proti vrhu menjavajo z roženci.

Naše delo potrjuje izvor primarnega vulkanoklastičnega zaporedja na območju Bloške planote in izključuje njegov epiklastičen oziroma presedimentacijo.

Introduction

The Borovnik Member, assumingly Carnian in age (Dozet 1979, 2002, this volume), forms a part of the Mohorje Formation (Fig. 1) which has been subdivided into four lithostratigraphic members, namely: Bošte Member, Borovnik Member, Rupe Member and Selo at Rob Member (Dozet 1979, 2002, this volume). The Mohorje Formation consists of carbonate, clastic and volcaniclastic rocks, and is underlain conformably by thickly-bedded and massive, mainly light grey carbonate rocks with numerous dasycladacean.

The Borovnik Member is named according to Borovnik hillock. The best outcroppings occur in a small and deep valley, the Borovnik Ravine. The sequence begins with a small rhyolitic lava flow that underwent mixing with wet unconsolidated silt. Overlying pyroclastics consist of bedded and laminated coarse- and fine-grained rhyolitic tuffs. The magma underwent strong fractionation; plagioclase and alkali feldspar phenocrysts

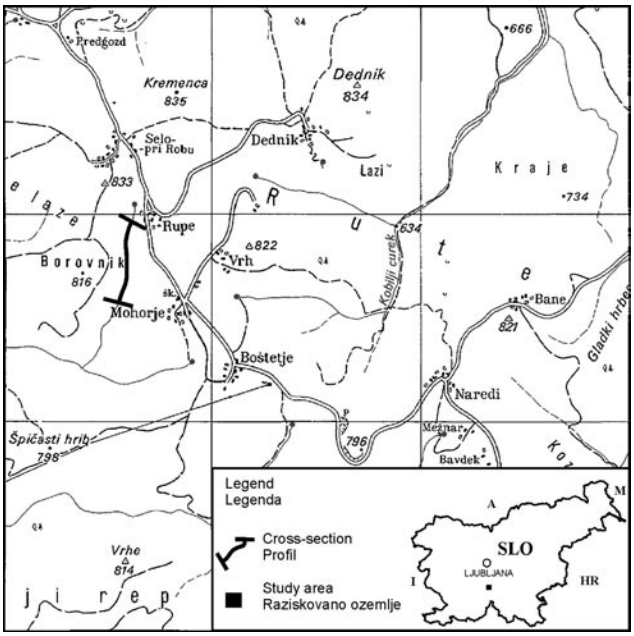

Fig. 1. Location map

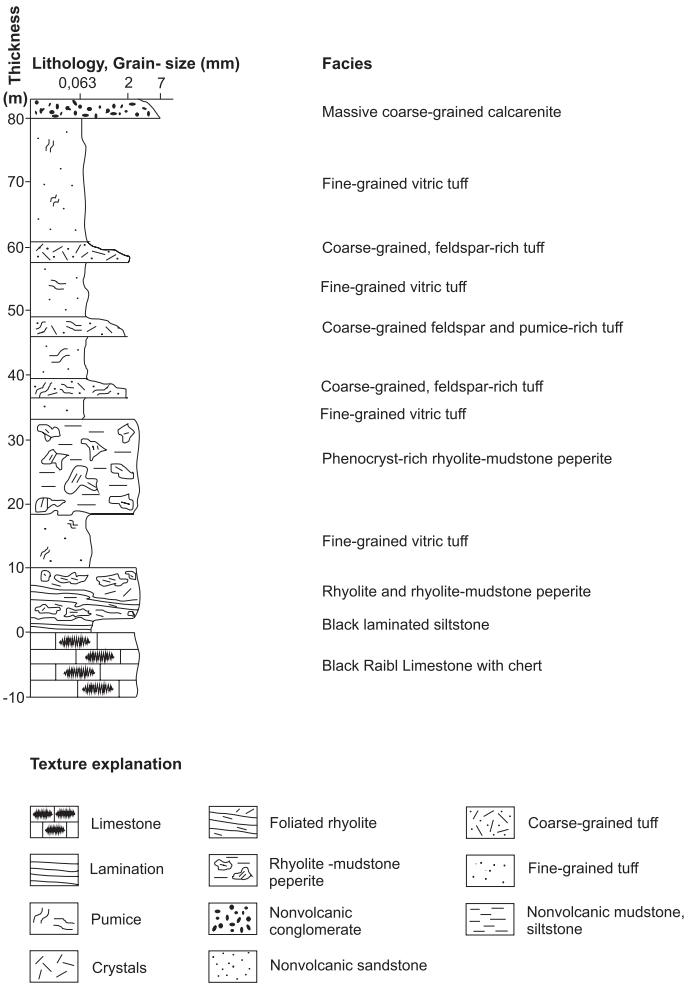

Fig. 2. Cross-section through the Borovnik Member volcanic and volcaniclastic succession

were accumulated in the late volcanic products and imparted them a dacitic character. The late-stage dacitic magmas were mainly emplaced as shallow intrusives and underwent mixing with unconsolidated surrounding sediments and tuffs producing dacite/siltstone and dacite/rhyolitic tuff peperites. The peperite composition depends on the quantity of admixed sediment and differs from dacitic composition in the abundance of major oxides and trace elements.

On the territory of Slovenia, the Ladinian epoch was the time of the most intensive volcanic activity during the Mesozoic era (Grafenauer, 1980, 1985; Grafenauer et al. 1983). For that reason, little attention has been paid to volcanic activity that occurs in Carnian sedimentary successions (Duhovnik, 1956; Buser & Hinterlechner-Ravnik, 1972; Dozet 1979, 2002, this volume). Our study confirms the existence of primary volcanic activity in the Bloke Plateau area and reveals the existence some lithostratigraphic types in the sequence which have not been identified yet.

Petrology of the Borovnik Member

Volcanic sequence (Fig. 2) is underlain by calcarenite composed of slightly recrystallised limestone lithic fragments. Cement is mainly calcite; besides that, up to 7 vol. % of brownish-yellow authigenic paragonite occur. Paragonite was seemingly developed upon thermal-contact metamorphosis related to volcanic activity. The calcarenite grades into dacite/siltstone peperite. The peperite is characterised by fluidal texture that resembles laminar structure composed of alternating glassy lava and siltstone. Siltstone is thermally metamorphosed and the primary constituents altered into iron oxides, mixed-layered clay minerals, quartz and albite. Fluidal texture was developed by laminar lava flow that incorporated silt and distributed it along the flow planes. The contacts of lava-siltstone laminae are commonly corroded. Authigenic minerals are slightly coarser than in the central parts and are up to 60 μm sized. Up to 100 μm wide veinlets are composed of fine-grained quartz.

The overlying pyroclastic sequence consists of bedded to laminated rhyolitic vitric tuffs ranging in grain-size from coarse- to fine-grained. In general, the trend of upward fining can be recognised. Lamination and bedding may be locally only faintly or vaguely. The tuff consists of rhyolite glass shards; coarser varieties may contain subordinate amounts of pumice. Plagioclase crystals are rare, too, and amount up to 10 vol. % of the bulk rock. Volcanic glass is extensively altered into microcrystalline quartz and albite, and filosilicates – mixed layered clay minerals and chlorite. Pyroclastic sequence terminates with fine-grained conglomerate. The grains are well-rounded to subangular and composed of quartzite. Cement consists of calcite and limonite. Pyroclastic sequence is intruded by dacite contaminated by siltstone. Dacite/siltstone peperite and dacite/rhyolitic tuff peperite developed. All rock varieties are extremely rich in plagioclase and potassium feldspar phenocrysts and indicate that they evolved from accumulates formed by crystal fractionation during magma development.

Dacite consists of phenocrysts of zonal, or more rarely, twinned plagioclases attaining the size up to 3 mm. They are replaced by fine-grained cloudy aggregates of albite which is slightly kaolinitized and sericitized. Potassium feldspars mainly belong to sanidine and they are relatively well preserved. Glassy groundmass is entirely altered into secondary minerals, mainly chlorite, iron oxides, quartz, albite, epidote, prehnite, and in some places calcite.

Peperite composition is also dominated by plagioclase and potassium feldspar phenocrysts, which have the same size and composition as in dacite. They are commonly corroded and characteristically cut by microfracture systems resulting from stress during magma intrusion into sediment and their mixing. The microfracture systems in phenocrysts are commonly filled by authigenic feldspar of the same composition as the phenocryst, or by quartz or iron oxides. Glassy groundmass and siltstone are mixed and extensively altered, mainly into iron oxides, chlorite, paragonite and quartz. In dacite/rhyolitic tuff peperite epidote, prehnite, quartz and albite also occur, but iron oxides are less extensively developed. Zircon grains partially originate from the zircons magma and partially from the siltstone. Zircons have broad reaction rims originating from radioactive decay, and show roundness, that could have been developed in several reworking cycles. Apatite originates from the magma, or partially from authigenic growth as a consequence of thermal metamorphosis.

Geochemistry of the Borovnik Member

Sixteen representative fresh rock samples were chosen for chemical analysis, which was performed at X-RAL Activation Services Inc., Don Mills, Ontario, by combined wet chemical method, ICP (Inductively Coupled Plasma Source), XRF (X-Ray Fluorescence), and MS (Mass Spectroscopy) to attain high analytical precision and reproducibility. The content of major and trace elements is shown in Tables 1, 2, and 3.

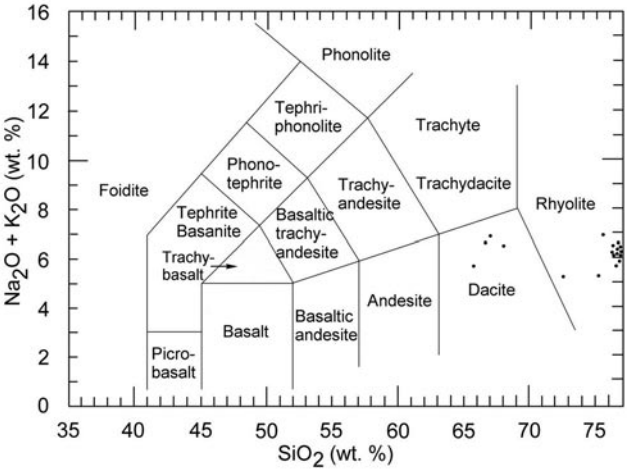

Fig. 3. Classification of the Borovnik Member volcanics in the alkali-silica diagram after Le Bas et al. 1986

The rocks have variable silica content ranging from 65,7 wt. % to 80,2 wt. % (recalculated on water-free basis). FeO_{tot} varies from 0,94 wt. % to 5,05 wt. %), and MgO from 0,48 wt. % to 1,39 wt. %; both oxides are appreciably enriched in contaminated dacite and dacite/siltstone peperite. Similarly broad variation and enrichment have been observed for alkali and alkaline earth metal oxides – CaO (0,12–4,25 wt. %), Na_2O (3,09–6,03 wt.%) and K_2O (0,65–2,82). In the TAS classification diagram (Le Bas et al. 1986), the samples are clustered into two groups occupying the dacite and rhyolite fields (Fig. 3). The majority of pyroclastic rocks shows rhyolitic affinity. The dacite composition of some samples arises from two main processes – fractional crystallization that caused accumulation of plagioclases and accessory minerals like zircon and apatite, and magma contamination with the sediment during the peperite formation.

Trace element abundance and some elemental ratios are displayed in Tables 2, 3 and 4. Incompatible trace elements range from 108,1–1118,2 ppm for Ba, 38,1-343,9 ppm for Sr and 14,9–176,6 ppm for Rb. Among compatible trace

Table 1. Major oxides (in wt. %)

Oxide/ Sample	No.	SiO_2	TiO_2	Al_2O_3	Fe_2O_3	MgO	CaO	MnO	Na_2O	K_2O	P_2O_5	TOT/C	TOT/S	Sum
GGS-10	**4**	64,53	0,08	18,62	2,76	0,72	3,19	0,04	4,65	1,64	0,08	0,26	1,25	99,81
GGS-11	**5**	63,69	0,07	18,15	4,45	1,07	3,36	0,06	4,55	1,03	0,07	0,16	1,31	99,8
GGS-12	**6**	78,07	0,03	12,15	1,42	0,51	0,2	0,01	6,03	0,25	0,03	0,06	0,03	99,76
GGS-13	**7**	66,31	0,07	18,21	2,48	0,91	3,04	0,03	4,06	1,64	0,07	0,08	0,84	99,75
GGS-14	**8**	64,59	0,07	18,65	2,28	0,8	4,25	0,03	4,95	1,22	0,07	0,38	0,67	99,78
GGS-15	**9**	72,98	0,04	13,76	1,97	0,99	1,9	0,01	3,09	1,96	0,04	0,18	0,02	99,79
GGS-16	**10**	79,2	0,02	11,81	1,14	0,58	0,08	<0,01	5,27	0,5	0,02	0,04	0,01	99,89
GGS-17	**11**	75,69	0,02	13,1	1,88	0,8	0,67	0,01	4,83	1,01	0,02	0,04	0,01	99,85
GGS-19	**12**	74,06	0,03	14,34	1,52	0,71	0,23	0,01	5,36	1,42	0,03	0,04	0,01	100,01
GGS-21	**13**	75,76	0,02	13,6	1,37	0,7	0,19	0,01	4,96	1,28	0,02	0,04	0,01	99,88
GGS-22	**15**	70,1	0,03	15,09	2,97	1,39	1,48	0,01	2,22	2,82	0,03	0,07	<0,01	99,83
GGS-23	**16**	76,7	0,02	12,83	1,59	0,8	0,12	0,01	5,38	0,74	0,02	0,03	<0,01	99,88
GGS-24	**17**	76,43	0,02	13,49	0,95	0,65	0,19	0,01	4,8	1,35	0,02	0,07	<0,01	99,88
GGS-28	**18**	75,89	0,02	13,34	1,24	0,75	0,51	0,01	5,23	0,9	0,02	0,12	<0,01	99,89
GGS-29	**19**	78,27	0,02	12,15	1,06	0,49	0,43	0,01	5,43	0,65	0,02	0,11	0,01	99,9
GGS-30A	**20**	77,59	0,02	12,78	0,84	0,48	0,33	0,01	5,29	0,87	0,02	0,08	<0,01	99,9

Table 2. Trace elements (in ppm)

Element/ Sample	No.	Ni	Sc	Ba	Be	Co	Cs	Ga	Hf	Nb	Rb	Sn	Sr	Ta
GGS-10	**4**	20	13	536,4	2	8,6	3,2	21,5	5,9	11,1	55,3	3	272,6	0,8
GGS-11	**5**	22	13	450,9	2	14,1	2,3	21,3	5,8	11,3	31,9	2	302,9	0,7
GGS-12	**6**	11	5	1198,2	1	19,3	0,5	13,1	4,9	11,5	14,9	7	57,6	1,3
GGS-13	**7**	11	13	761,1	3	10,5	5,2	21,4	6,4	13,1	70,6	3	311,6	0,9
GGS-14	**8**	12	15	683,4	3	8,8	2,6	21,2	7,3	14,3	43,8	2	343,9	0,8
GGS-15	**9**	16	8	639,2	3	6,9	6,1	16,5	5,3	12,3	116,5	6	211,5	1,0
GGS-16	**10**	9	4	122,8	2	17,5	0,9	13,6	4,6	10,6	33,8	6	38,3	1,3
GGS-17	**11**	10	6	324,8	2	10,4	2,6	14,9	5,4	12,0	56,4	6	118,2	1,2
GGS-19	**12**	6	6	284,3	4	7,3	3,2	18,9	5,9	13,3	85,0	8	57,5	1,3
GGS-21	**13**	12	5	269,6	4	14,4	3,1	16,5	5,0	12,0	81,6	7	60,5	1,3
GGS-22	**15**	<5	10	480,2	4	4,5	8,5	20,1	6,2	13,5	176,6	6	136,2	1,1
GGS-23	**16**	6	5	169,7	3	15,2	1,4	16,6	5,0	11,9	47,1	7	53,6	1,3
GGS-24	**17**	6	5	198,1	3	9,5	2,2	19,3	5,1	12,3	85,0	8	45,3	1,3
GGS-28	**18**	7	5	160,7	4	11,5	1,7	16,4	4,7	12,2	50,1	7	39,8	1,2
GGS-29	**19**	5	4	108,1	2	10,6	1,2	12,8	4,3	10,9	37,3	6	39,1	1,1
GGS-30A	**20**	<5	5	133,0	3	21,3	1,4	15,2	4,6	11,6	49,3	7	38,1	1,2

Table 2. – Continuation

Element/ Sample	No.	Th	U	W	Zr	Mo	Cu	Pb	Zn	Ni	As	Hg
GGS-10	**4**	17,6	3,1	134,6	221,9	0,7	2,6	22,6	24	0,8	13,3	0,02
GGS-11	**5**	16,1	2,4	171,3	229,3	0,7	2,4	24,0	30	0,8	13,0	0,06
GGS-12	**6**	23,7	9,7	252,2	130,2	0,1	1,5	59,4	51	0,6	2,,2	0,05
GGS-13	**7**	19,9	3,4	159,6	240,6	0,3	2,3	21,0	21	0,8	10,6	0,05
GGS-14	**8**	18,7	5,2	149,8	285	0,4	2,5	20,2	33	0,7	10,4	0,05
GGS-15	**9**	23,3	5,1	103,4	171,1	0,1	1,5	42,4	32	0,1	<0,5	0,02
GGS-16	**10**	22,1	9,2	339,2	115,7	0,1	4,8	6,7	28	0,4	2,5	0,03
GGS-17	**11**	21,2	6,3	215,4	158,8	0,2	3,1	21,8	42	0,3	1,5	0,06
GGS-19	**12**	27,3	7,5	136,5	159,0	0,1	1,8	2,2	36	0,2	2,5	0,04
GGS-21	**13**	25,6	8,5	196,2	132,7	0,1	1,7	4,0	36	0,3	1,8	0,06
GGS-22	**15**	23,5	4,5	63,0	199,9	<0,1	1,0	3,7	38	0,2	1,6	0,01
GGS-23	**16**	24,4	6,0	220,1	132,0	0,1	1,3	50,0	50	0,3	2,0	0,06
GGS-24	**17**	25,2	5,4	181,2	130,9	0,1	2,3	4,1	19	0,4	2,0	0,05
GGS-28	**18**	24,1	7,1	157,1	124,0	0,1	8,1	9,4	40	1,2	4,1	0,05
GGS-29	**19**	23,7	7,2	173,6	114,7	0,1	4,3	4,5	27	0,9	2,8	0,05
GGS-30A	**20**	22,7	6,1	259,1	121,4	0,1	2,4	4,3	23	0,6	2,7	0,05

Table 3. REE elements (in ppm)

Element/ Sample	No.	Y	La	Ce	Pr	Nd	Sm	Eu	Gd	Tb	Dy	Ho	Er	Tm	Yb	Lu
GGS-10	**4**	22,9	81,8	170	17,66	61,9	8,89	2,08	5,40	0,87	4,03	0,74	2,10	0,32	2,06	0,31
GGS-11	**5**	26,0	51,0	110,1	11,46	41,1	6,16	2,09	4,64	0,84	4,30	0,88	2,48	0,38	2,53	0,39
GGS-12	**6**	36,9	36,3	85,3	9,81	36,7	7,43	0,67	5,94	1,17	5,99	1,17	3,46	0,54	3,63	0,54
GGS-13	**7**	23,4	87,0	181,6	19,08	68,0	9,79	2,20	6,15	1,00	4,62	0,79	2,17	0,31	2,19	0,32
GGS-14	**8**	34,3	92,6	191,0	20,24	72,1	10,53	2,53	7,28	1,23	5,94	1,10	3,09	0,47	3,10	0,48
GGS-15	**9**	37,7	58,5	127,8	14,29	51,0	9,02	1,23	6,78	1,27	6,27	1,15	3,21	0,47	3,22	0,46
GGS-16	**10**	35,4	32,2	75,9	8,90	32,4	6,70	0,68	5,41	1,05	5,61	1,09	3,13	0,49	3,27	0,49
GGS-17	**11**	37,5	46,0	100,9	11,62	42,2	7,91	0,94	6,29	1,22	6,22	1,20	3,38	0,53	3,45	0,51
GGS-19	**12**	42,4	40,3	91,6	10,78	40,9	8,09	0,65	6,56	1,31	6,94	1,31	3,97	0,61	4,19	0,62
GGS-21	**13**	38,9	37,7	83,8	10,12	38,5	7,60	0,59	6,05	1,21	6,22	1,23	3,68	0,59	3,98	0,60
GGS-22	**15**	38,7	66,1	137,9	15,64	56,2	9,90	1,29	7,53	1,38	7,00	1,23	3,25	0,48	3,12	0,46
GGS-23	**16**	38,6	38,1	85,4	9,94	37,6	7,51	0,59	6,21	1,28	6,56	1,25	3,63	0,55	3,74	0,56
GGS-24	**17**	38,1	30,5	70,6	8,20	29,5	6,24	0,50	5,11	1,15	6,24	1,25	3,72	0,59	3,99	0,60
GGS-28	**18**	58,9	49,5	89,7	13,22	52,2	11,41	0,94	10,22	1,99	9,51	1,84	5,12	0,75	5,03	0,76
GGS-29	**19**	43,6	37,4	78,1	10,00	38,7	7,84	0,65	6,99	1,37	6,80	1,32	3,84	0,61	3,99	0,59
GGS-30A	**20**	37,9	37,3	75,1	9,75	36,4	7,52	0,67	6,11	1,24	6,43	1,21	3,51	0,55	3,67	0,52

Table 4. Some elemental ratios

Oxide/ Sample	No.	La_{PAAS}/Yb_{PAAS}	La_{PAAS}/Sm_{PAAS}	Gd_{PAAS}/Yb_{PAAS}	Eu/Eu_{Ch}*	Th/U	Zr/Nb	La_{Ch}/Yb_{Ch}	La_{Ch}/Sm_{Ch}	Gd_{Ch}/Yb_{Ch}
GGS-10	**4**	2,93	1,34	1,59	0,92	5,68	20,01	26,83	6,46	2,12
GGS-11	**5**	1,49	1,20	1,11	1,07	6,71	20,29	13,62	5,21	1,49
GGS-12	**6**	0,74	0,71	0,99	0,55	2,44	11,32	6,83	3,08	1,38
GGS-13	**7**	2,93	1,29	1,70	0,90	5,85	18,37	26,83	5,59	2,28
GGS-14	**8**	2,21	1,28	1,42	0,92	3,60	19,93	20,19	5,54	1,90
GGS-15	**9**	1,34	0,94	1,27	0,68	4,57	13,91	12,28	4,08	1,71
GGS-16	**10**	0,73	0,70	1,00	0,58	2,40	10,92	6,67	3,03	1,34
GGS-17	**11**	0,98	0,84	1,10	0,63	3,37	13,23	9,01	11,60	1,48
GGS-19	**12**	0,71	0,72	0,95	0,51	3,64	11,95	6,50	3,14	1,27
GGS-21	**13**	0,70	0,72	0,92	0,51	3,01	11,04	6,40	3,12	1,23
GGS-22	**15**	1,56	0,97	1,46	0,66	5,22	14,81	14,32	3,10	1,21
GGS-23	**16**	0,75	0,74	1,00	0,51	4,07	11,09	6,88	3,19	1,35
GGS-24	**17**	0,56	0,71	0,78	0,51	4,67	10,64	5,17	3,08	1,04
GGS-28	**18**	0,73	0,63	1,23	0,51	3,39	10,16	6,65	2,72	1,65
GGS-29	**19**	0,69	0,69	1,06	0,51	3,29	10,52	6,33	3,00	1,42
GGS-30A	**20**	0,75	0,72	1,01	0,54	3,72	10,47	6,87	3,12	1,35

PAAS normalization – Post Archean Australian Shale (Taylor & McLennan, 1985; **Ch** normalization - chondritic values after Nakamura, 1974)

elements, Ni displays a trend of decrease with the increasing silica content from maximum 22 ppm in dacite to <5 ppm in rhyolite. Sc varies from 4 ppm to 15 ppm, and shows similar decreasing trend with increasing SiO_2 (Fig. 4). V ranges from 20 ppm in dacites and dacite/siltstone peperites to <5 ppm in rhyolites. The content of TiO_2 ranges from 0,08 wt.% in rhyolites to 0,27 wt. % in dacites and dacite/siltstone peperites, and this trend is identical to that for Sc (Fig. 4). There is a similar, but unexpected trend of decreasing Zr abundance with increasing silica (Fig. 4) – from 114,7 ppm in rhyolite to 285 ppm in dacite. In daci-te and dacite/siltstone peperite, zircon grains are well seen. Some of them seem to have igneous origin, but the others have broad dark margins and rounded form, originated very possibly from sedimentary rocks, maybe from several reworking cycles even. Nb variations are scattered and range from 10,6 ppm 14,3 ppm. The shows a consistent trend of increase with increasing silica (Fig. 4); for U the trend is about the same but the values are more scattered than for Th, what can be seen from the diagram Zr/Nb vs Th/U (Fig. 4).

Chondrite (Ch) normalized abundance (after Nakamura, 1974) of the analysed samples is about 100 times higher for LREEs, and about 10 times higher for HREEs than chondritic values. Rare earth elements (REEs) show fractionation and contamination processes. Fractionation of plagioclases is reflected in more extreme negative europium anomalies (Eu/Eu*) for rhyolitic rocks (0,51–0,58) than for dacitic rocks (0,68–0,92). Contamination with the sediment is best shown in the opposite trends of LREEs and HREEs with chondrite normalized samples. The sediment is enriched with LREEs which is the cause for unusual virtual decrease of LREEs with increased silica (Fig. 4). That is also reflected in the La_{PAAS}/Yb_{PAAS} (PAAS – Post Archean Australian Shale, after Taylor & Mclennan, 1985) and La_{Ch}/Yb_{Ch} (Ch – chondrite, after Nakamura, 1974) ratios (Table 4) which are relatively consistent for rhyolitic pyroclastic rocks (0,49–0,73), but variable for contaminated dacites and dacite/siltstone peperites (1,34 – 2,93). Similar relation can be observed for the La_{PAAS}/Sm_{PAAS} and La_{Ch}/Sm_{Ch} ratios ranging from 0,63–0,74 for rhyolites and from 0,94–1,29 for dacitic rocks. Yttrium, as expected, follows the trend of HREEs and increases with the increase in silica (Fig. 4).

Conclusions

About 230 metres thick Julian and Tuvalian (Middle and Upper Carnian) Mohorje Formation in the Bloke Plateau area comprises a 75 m thick Borovnik Member composed of volcanic and volcaniclastic rocks deposited in a shallow-marine environment. Volcanic activity started with an extrusion of a minor rhyolitic lava flow that underwent mixing with the enclosing silty sediment. Rhyolite/dacite peperite with flow structure developed. The lava extrusion was followed by a vigorous explosive volcanic activity that produced coarse- and fine-grained vitric tuffs of rhyolitic composition. The tuffs are bedded and laminated and form a fining-upward sequence. Coarser-grained tuffs commonly contain some pumice lapilli.

Magmas producing the pyroclastic sequence were strongly fractionated, and a great part of plagioclase and alkali feldspar phenocrysts had been removed from the melt in the time of extrusion. The magma with accumulated phenocrysts erupted the latest, and was emplaced into wet unconsolidated sediments and tuffs as a shallow or subsurface body. The dacite composition is related to the phenocryst separation from rhyolitic or rhyodacitic magma. The "dacite" composition is also observed for the peperite samples, but in a

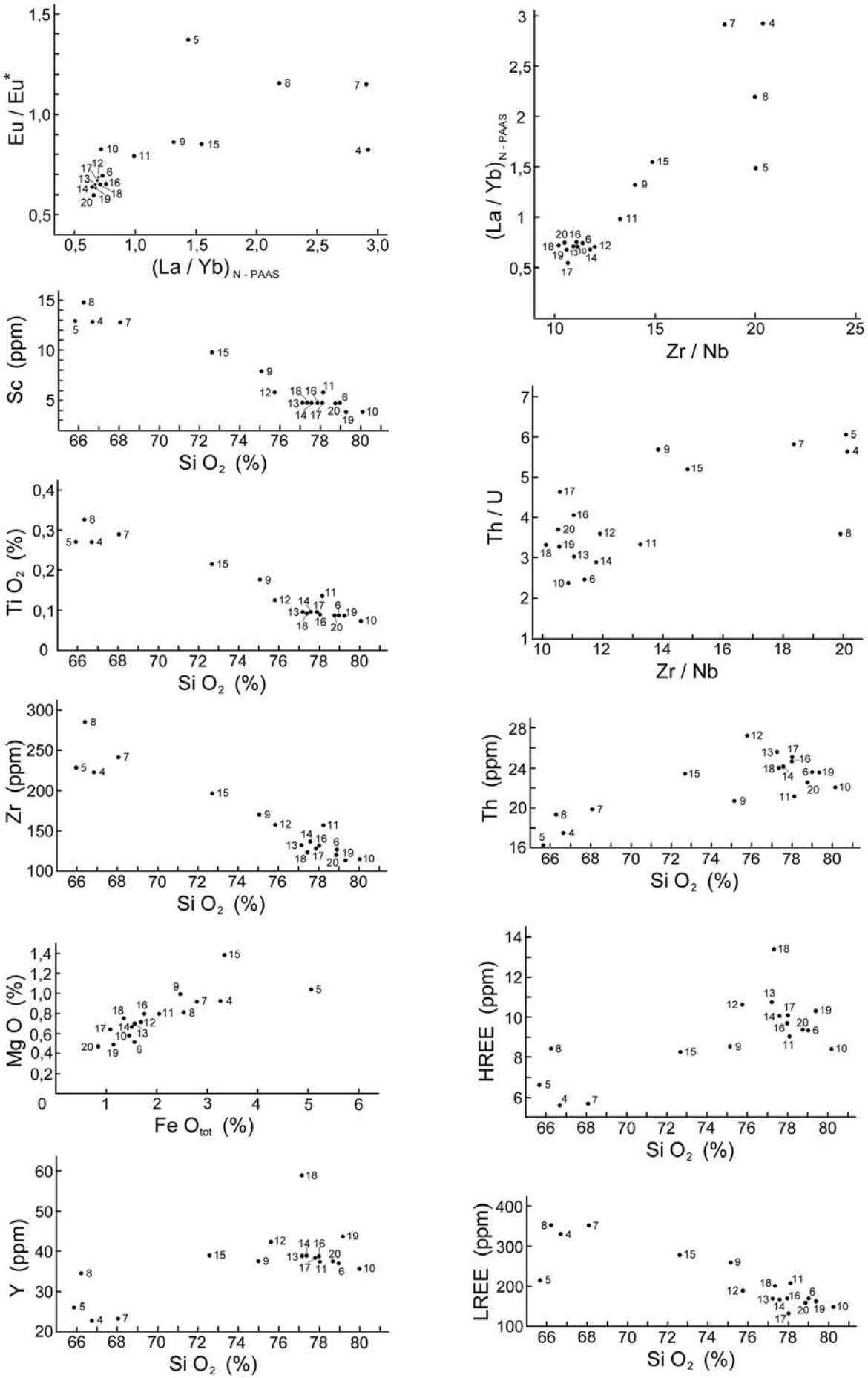

Fig. 4. Some elemental (oxide) ratios for the Borovnik Member Volcanics (N-PAAS, normalization to PAAS values, Eu/Eu* europium anomaly based on chondritic values of Nakamura, 1974, and calculated after proposal of Taylor & McLennan, 1985).

more extreme way owing to more siltstone component admixed. External water originating from the enclosing sediments and/or tuffs and the heat from shallow intrusive body developed ephemeral hydrothermal conditions reflected in extensive alteration of the groundmass, tuff and siltstone peperite matrix. The most abundant authigenic minerals are iron oxides, filosilicates, quartz and albite, although epidote and prehnite also occur particularly in the dacite/rhyolitic tuff peperite.

Acknowledgements

Our work was granted by Slovenian Research Agency, Programmes P1-0011 and P1-0025. We are kindly acknowledged to Dr. Bogomir Celarc for reviewing the manuscript.

References

Buser, S. & Hinterlechner-Ravnik, A. 1972: Sledovi karnijskega vulkanizma v južni Sloveniji. 7. Geol. Kongr. Savez. geol. društ. Jugosl. (Zagreb) 1: 113–119.

Dozet, S. 1979: Karnijske plasti južno in zahodno od Ljubljanskega barja **(***Carnian beds south and west of the Ljubljana Moor*). Geologija (Ljubljana) 22/1: 55–70.

Dozet, S. 2002: Grosupeljsko-Orelske paralično-plitvovodne plasti (*Grosuplje-Orle paralic-shallow water beds*). RMZ, Mater. & Geoenvir. (Ljubljana) 49/4: 571–591.

Dozet, S. 2009: Mohorje Formation, Southern Slovenia. Geologija (Ljubljana), 52/1: this volume.

Duhovnik, J. 1956: Pregled magmatskih in metamorfnih kamenin Slovenije (*Review of igneous and metamorphic rocks in Slovenia*). Prvi jugosl. geol. kongr. (Ljubljana) 1: 23–26.

Grafenauer, S. 1980: Petrologija triadnih magmatskih kamnin na Slovenskem (*Petrology of Triassic igneous rocks in Slovenia*). Razprave 4. razr. SAZU (Ljubljana) 25: 1–220.

Grafenauer, S. 1985: Nastanek triasnih magmatskih kamnin na Slovenskem (*Origin of Triassic igneous rocks in Slovenia*). Razprave 4. razr. SAZU (Ljubljana) 26: 387–400.

Grafenauer, S., Duhovnik, J. & Strmole, D. 1981: Magmatske kamnine v zahodnih Karavankah (*Igneous rocks in Western Slovenia*). Rud. met. zbornik (Ljubljana) 28/2–3: 127–150.

Grafenauer, S., Duhovnik, J. & Strmole, D. 1983: Triadne magmatske kamnine vzhodne Slovenije (*Triassic igneous rocks of Eastern Slovenia*). Geologija (Ljubljana) 26: 189–241.

Le Bas, M.J., LeMaitre, R. W., Streckeisen, A. & Zanettin, B. 1986: A chemical classification of volcanic rocks based on total alkali-silica diagram. J. Petrology (Oxford) 27: 745–750.

Nakamura, N. 1974: Determination of REE, Ba, Fe, Mg, Na and K in carbonaceous and ordinary chondrites. Geochim. Cosmochim. Acta (Amsterdam) 38: 757–775.

Taylor, S. R. & McLennan, S. M. 1985: The continental crust: Its composition and evolution. Blackwell Scientific Publications, 1–186.